Temperature Effects on Excitation Relaxation Dynamics of the Carotenoid β-Carotene and Its Analogue β-Apo-8′-carotenal, Probed by Femtosecond Fluorescence Spectroscopy†

Seiji Akimoto,‡ Iwao Yamazaki,‡ Takahiro Sakawa,§ and Mamoru Mimuro*,§

Department of Molecular Chemistry, Graduate School of Engineering, Hokkaido University, Sapporo 060-8628, Japan, and Department of Physics, Biology and Informatics, Faculty of Science, Yamaguchi University, Yamaguchi 753-8512, Japan

Received: July 6, 2001; In Final Form: January 16, 2002

Femtosecond time-resolved fluorescence spectra were measured on the carotenoid β-carotene and its analogue β-apo-8′-carotenal in 2-methyltetrahydrofuran at 295 and 80 K. β-Carotene showed intramolecular vibrational redistribution (IVR) with time constants of 40−80 fs depending on the wavelengths, followed by vibrational relaxation with a time constant of 220 fs. At 80 K, the former process was resolved; however, the latter was not necessarily clear because of large spectral changes. However, β-apo-8′-carotenal showed relaxation processes different from those of β-carotene; the IVR process was not resolved under both temperature conditions, and at 80 K, the decay constants were prolonged at all wavelengths measured. Changes in the time-resolved fluorescence spectra were discernible but small. These findings indicate that the IVR process of β-apo-8′-carotenal was very fast, that it was shorter than our time resolution (30 fs), and that the slow relaxation process involved an interaction between a solute and a solvent, especially under the low-temperature condition.

1. Introduction

Electronic spectroscopy and excited-state dynamics of linear polyenes and carotenoids continue to be topics of considerable interest because of their important functions. Carotenoids have several kinds of biological activities, such as radical scavenging, singlet oxygen trapping, and other protective activities.[1−3] In photosynthesis, carotenoids have an additional function: they absorb light energy and transfer it to a photochemical reaction center where a light-induced electron-transfer reaction takes place. Two kinds of carotenoids are found in photosynthetic organisms; one consists of conjugated polyenes (−(C═C)$_n$−) and the other contains a keto carbonyl group (>C═O) in the conjugated double-bond system. It is well-known that the carotenoids in the latter group, such as fucoxanthin and peridinin, work as efficient antenna pigments.[4,5] In the case of peridinin, its excitation relaxation dynamics and its energy-transfer pathway to chlorophyll have received much attention because of its unique molecular structure and the unique crystal structure of the pigment−protein complex.[5−7]

Carotenoids are, in general, classified as polyenes belonging to the point group C_{2h} in which two energetically low-lying singlet states are expected. One is closely related to the 2Ag (S_1) state, which is dipole forbidden from the ground (S_0) state by parity, and the other is related to the 1Bu (S_2) state, which is allowed for one-photon excitation.[8] According to this assignment, the relaxation processes of carotenoids are expected to be as follows: optical excitation to the S_2 state induces an internal conversion to the S_1 state followed by relaxation to the ground state. Besides the above-described electronic relaxation, intramolecular vibrational redistribution (IVR) and vibrational relaxation (VR) occur in each electronic state. Because of the presence of the two singlet excited states, two energy-transfer pathways are possible in the photosynthetic antenna system: one from the S_2 state of the carotenoids to the S_2 state of (bacterio)-chlorophylls, and the other from the S_1 state of the carotenoids to the S_1 state of (bacterio)chlorophylls. The energy-transfer pathway is closely related to the molecular structure of carotenoids. Both pathways are operative for carotenoids of conjugated polyenes in bacterial antenna,[9−12] whereas only the latter is active for carotenoids with a keto carbonyl group.[4,5] Because energy transfer is a competitive process with other relaxation processes, it is critical to understand the excitation relaxation kinetics within carotenoid molecules.

The initial relaxation processes of carotenoids have been recently investigated from several points of view using ultrafast time-resolved fluorescence.[5,12−18] Fleming and co-workers examined the internal conversion and energy transfer dynamics of spheroidene in solution and in the LH1 and LH2 complexes of photosynthetic bacteria.[12] Macpherson and Gillbro investigated the solvent dependence of the $S_2 \rightarrow S_1$ internal conversion rate of β-carotene.[14] Recently, we examined (1) the effects of molecular structures on the S_2-state dynamics of β-carotene and its analogues[15] and two stereochemical forms (all-*trans* and 9′-*cis*) of neoxanthin,[16] (2) the IVR and VR within the S_2 state of neurosporene,[17] and (3) the $S_2 \rightarrow S_1$ internal conversion for the linear carotenoids as a function of the conjugation length (n = 5−13).[18] We showed that the rate constants of internal conversion were not monotonically related to the conjugation length. Thus, there is still some unknown factor(s) involved in relaxation processes.

In the present study, we report the temperature effect on ultrafast dynamics of β-carotene and β-apo-8′-carotenal probed by femtosecond (fs) fluorescence spectroscopy. Under the low-temperature condition, the movement of the solute and solvents is restricted compared with the situation in solutions, and this is analogous to the case in pigment−protein complexes. β-Carotene consists of nine conjugated double bonds in the

† Part of the special issue "Noboru Mataga Festschrift".

* To whom correspondence should be addressed. Tel and Fax: +81-83-933-5725. E-mail: mimuro@mail.sci.yamaguchi-u.ac.jp.

‡ Hokkaido University.

§ Yamaguchi University.

10.1021/jp0125653 CCC: $22.00
Published on Web 02/08/2002

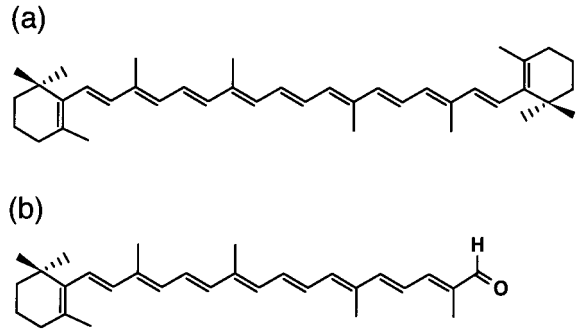

Figure 1. Molecular structures of (a) β-carotene and (b) β-apo-8′-carotenal.

central part with additional conjugations of two β-end groups, whereas β-apo-8′-carotenal is a carotenoid analogue that consists of eight conjugated double bonds with a keto carbonyl group at one end and a β-end group at the other end (Figure 1). We discuss the relaxation dynamics after excitation with large excess energy in relation to temperature and the molecular structure of these carotenoids.

2. Experimental Section

β-Carotene and β-apo-8′-carotenal were purchased from Wako Chemicals (Osaka, Japan) and Fluka (Switzerland), respectively. The β-carotene was purified by recrystallization (twice), and the β-apo-8′-carotenal was purified by HPLC fractionation. Their purity was checked by HPLC with a reverse-phase column (Nova-Pac C18, Waters, USA). 2-Methyltetrahydrofuran (MTHF) was purchased from Merck (Germany) and was used after distillation. The MTHF was not frozen even at 80 K.

Fluorescence rise and decay curves were measured with a femtosecond fluorescence up-conversion system, and the procedure was performed using a Ti:sapphire laser (Tsunami, Spectra-Physics, USA), pumped with a diode-pumped solid-state laser (Millennia Xs, Spectra-Physics, USA).[17−19] The IR pulses (840 nm, 80 MHz) were separated into two pulses; one was doubled by a BBO crystal (CASIX, China) and the second harmonic (420 nm) was used to excite samples, while the other IR beam served as a gate pulse. The gate pulse traversed a variable delay before being combined with the fluorescence in a 0.5 nm thickness BBO crystal (CASIX, China) in the type-1 phase-matching geometry, while the excitation pulse traversed a fixed delay before being focused into a temperature-controlled sample cell. To avoid polarization effects, the angle between polarizations of the excitation beam and the probe beam was set to the magic angle by a $\lambda/2$ plate (Sigma Koki, Japan). The excitation at 420 nm corresponds to the $S_0 \rightarrow S_2$ transition with excess energies of approximately 3000 cm^{-1} for β-carotene at 295 K, 4000 cm^{-1} for β-carotene at 80 K, 3300 cm^{-1} for β-apo-8′-carotenal at 295 K, and 4300 cm^{-1} for β-apo-8′-carotenal at 80 K.

After recording the time evolution of fluorescence at different wavelengths, the time-dependent fluorescence emission spectra were reconstructed as described elsewhere.[17,19] For all wavelengths, the integrated intensities of the fluorescence rise and decay curves were normalized to the steady-state fluorescence spectra. The fluorescence rise and decay curves were measured in the wavelength region from 470 to 580 nm with an interval of 10 nm and from 580 to 640 nm with an interval of 20 nm. Each decay curve was individually fit to a single- or double-exponential function using an iterative deconvolution method. A Gaussian function fitted to the up-conversion signal from the pure solvent Raman scattering was used as an instrumental response function. The temporal width of the instrument response was estimated to be 260 fs at 295 K and 270 fs at 80 K.

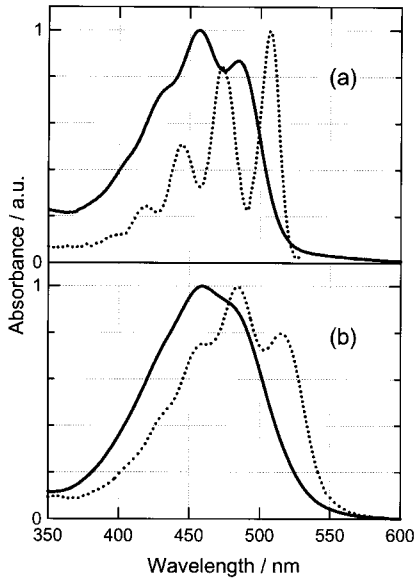

Figure 2. Normalized absorption spectra of carotenoids in MTHF at 295 K (solid lines) and 80 K (broken lines): (a) β-carotene; (b) β-apo-8′-carotenal.

For the time-resolved fluorescence measurements, a sample solution ($\sim 10^{-5}$ M) was placed in a cell with a 2-mm path length, which was mounted in a He cryostat (PS24SS, Daikin, Japan). The sample's temperature was monitored and controlled by a microprocessor-based digital temperature indicator/controller (9600, Scientific Instruments, USA). All measurements were carried out at 295 or 80 K. The steady-state fluorescence spectra were measured with a Hitachi F-4500 spectrofluorometer, and for the low-temperature spectra, a 10-mm quartz cell was settled in a custom-made Dewar bottle.

3. Results

Figure 2 shows the absorption spectra of β-carotene and β-apo-8′-carotenal in MTHF. Both compounds exhibit broad absorption spectra having maximum intensities of the $S_{0,0} \rightarrow S_{2,1}$ bands at 295 K. These diffuse spectra were caused by conjugation with the two β-end groups for β-carotene and with the keto carbonyl group for β-apo-8′-carotenal.[20−22] By contrast, at 80 K the absorption spectra show a vibronic structure and a maximum was shifted to the red by 20−30 nm. It is reported that the $S_0 \rightarrow S_2$ transition energy of carotenoid is linearly decreased with increasing solvent polarizability, which is calculated as $(n^2 - 1)/(n^2 + 2)$ where n is the refractive index.[23] By using refractive index values of MTHF at 94 K (1.73) and 298 K (1.41),[24,25] the polarizability ($(n^2 - 1)/(n^2 + 2)$) was determined to be 0.25 at 298 K and 0.40 at 94 K. On changing the polarizability from 0.25 to 0.40, the $S_0 \rightarrow S_2$ transition energy was expected to shift to lower by 1400 cm^{-1}, corresponding to approximately 30 nm at 450 nm. Therefore, the observed spectral shift was probably due to the higher solvent polarizability at the lower temperature. Compared with the absorption spectrum of β-carotene, that of β-apo-8′-carotenal was broad even at 80 K, indicating that its electronic structure was strongly characterized by conjugation with the keto carbonyl group. Because the energy level of the S_1 state of carotenoids is almost insensitive to environmental polarizability,[26] the energy

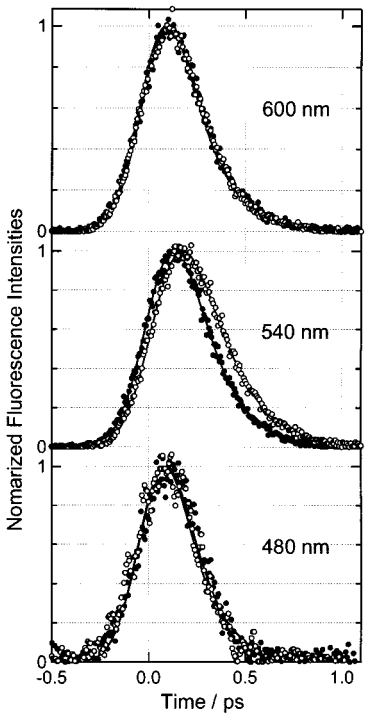

Figure 3. Fluorescence rise and decay curves of β-carotene at 295 K (○) and 80 K (●) in MTHF and the best-fit function (solid lines).

TABLE 1: Kinetic Parameters of the S_2 States in β-Carotene and β-Apo-8′-carotenal in MTHF[a]

	β-carotene		β-apo-8′-carotenal	
λ (nm)	295 K	80 K	295 K	80 K
480	155 (−)	120 (−)	70 (−)	135 (−)
510	150 (40)	130 (−)	135 (−)	150 (−)
540	150 (55)	140 (110)	130 (−)	180 (−)
580	165 (−)	155 (85)	150 (−)	225 (−)
640	160 (−)	175 (−)	180 (−)	255 (−)

[a] The numbers in parentheses indicate the rise times for the best fit of the observed rise and decay curves. Minus signs indicated the absence of a rise component.

gap between the S_2 and S_1 states is expected to decrease at a lower temperature. Besides the red-shift, a peak alteration was observed for the spectrum of β-carotene; the $S_{2,0}$ band increased its intensity at 80 K, suggesting that the displacement of potential surfaces between the S_0 and S_2 states of β-carotene was small under the low-temperature condition. In the case of β-apo-8′-carotenal, however, the $S_{2,1}$ band was strongest under both temperature conditions, suggesting that the displacement of the potential surfaces almost remained the same.

Figure 3 shows the fluorescence rise and decay curves of β-carotene at both 295 and 80 K. The fluorescence decay lifetimes were dependent upon the wavelengths monitored (Table 1); typically, the lifetimes were 135 fs for 480 nm, 145−150 fs for 500−560 nm, and 160−170 fs for 570−640 nm at 295 K. At 80 K, the lifetimes were resolved to 120 fs for 480−500 nm, 130−140 fs for 510−580 nm, and 160−190 fs for 600−640 nm. The estimated lifetimes were similar to each other, and longer lifetimes were resolved in the longer wavelength region under both temperature conditions. Besides the decay component, a rise component was necessary for the best fit of the fluorescence kinetics; at 295 K, the rise times of 40 and 80 fs were resolved at 510 and 560 nm, respectively, where the $S_{2,n} \rightarrow S_{0,n+1}$ or $S_{2,n} \rightarrow S_{0,n+2}$ transition corresponded. The presence of the rise time was consistent with the previous report.[17] At 80 K, the rise times were 85 and 110 fs at 580 and 540 nm, respectively. This wavelength region corresponded to the $S_{2,n} \rightarrow S_{0,n+1}$ or $S_{2,n} \rightarrow S_{0,n+2}$ transition. A prolonged rise time at 80 K was a kinetic feature for β-carotene.

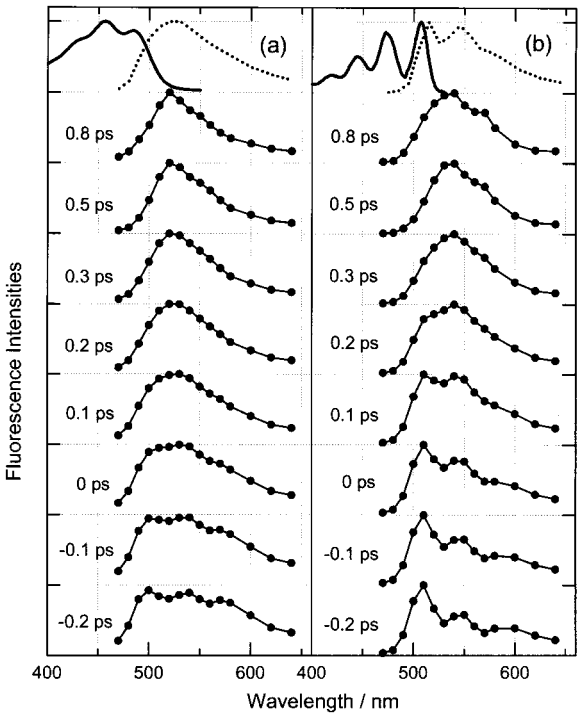

Figure 4. Normalized time-resolved fluorescence spectra of β-carotene at (a) 295 K and (b) 80 K in MTHF. The steady-state absorption (full lines) and fluorescence spectra (broken lines) at the respective temperatures are also shown in the upper window.

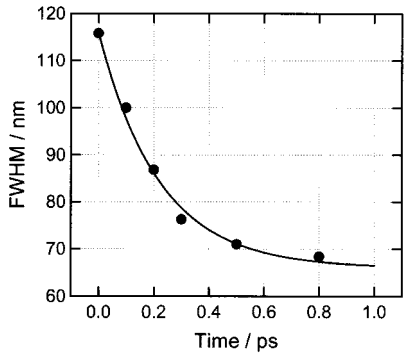

Figure 5. Changes in the bandwidth of the fluorescence spectrum of β-carotene as a function of the delay time at 295 K.

To examine temperature effects on the relaxation dynamics in the excited state of β-carotene, the time-resolved fluorescence spectra were obtained after normalization and are shown together with the steady-state absorption and fluorescence spectra (Figure 4). The transient spectrum at 295 K was diffuse upon initial excitation and decreased in width as the delay time increased. The wavelength dependence of fluorescence kinetics and the temporal evolution of fluorescence spectra of β-carotene were consistent with those observed for neurosporene, a linear carotenoid with a conjugation length of nine,[17] which is characteristic of the excitation relaxation of carotenes at 295 K. Figure 5 shows changes in the fluorescence bandwidth of β-carotene at 295 K as a function of the delay time. The solid line is the best-fit function of a single-exponential decay with a time constant of approximately 220 fs. This time constant was in good agreement with that obtained for tetradesmethyl-β-carotene, 253 fs,[27] and neurosporene, 210−260 fs,[17] and was then attributed to the VR (Table 2).

TABLE 2: Relationship between Relaxation Processes and Expected Observations in Fluorescence Kinetics and Spectra

relaxation process	fluorescence rise and decay curves	fluorescence spectra
IVR (from Franck−Condon active mode)	rise component at the middle of the spectral region	peak alternation
IVR (to dark mode)		loss of fine structure
displacement of potential surface	wavelength-dependent lifetime	spectral shift
VR	wavelength-dependent lifetime	spectral narrowing
internal conversion	decay of upper state and rise of lower state	spectral alternation

[a] Samples were restricted to carotenoids with β-end group(s) in MTHF after excitation to the S_2 state with an excess energy, as were analyzed in the present study. IVR and VR stand for intramolecular vibrational redistribution and vibrational relaxation, respectively.

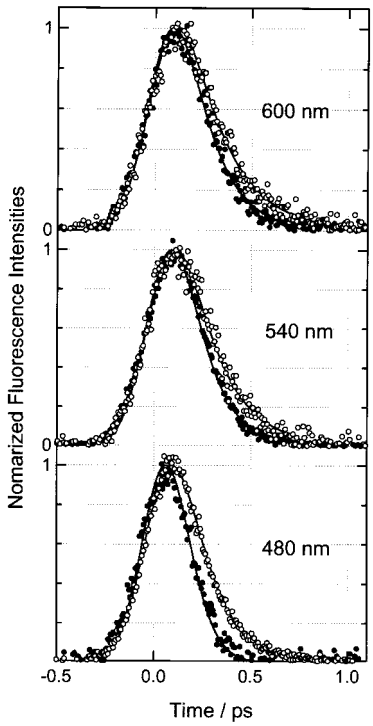

Figure 6. Fluorescence rise and decay curves of β-apo-8′-carotenal at 295 K (○) and 80 K (●) in MTHF and the best-fit function (solid lines).

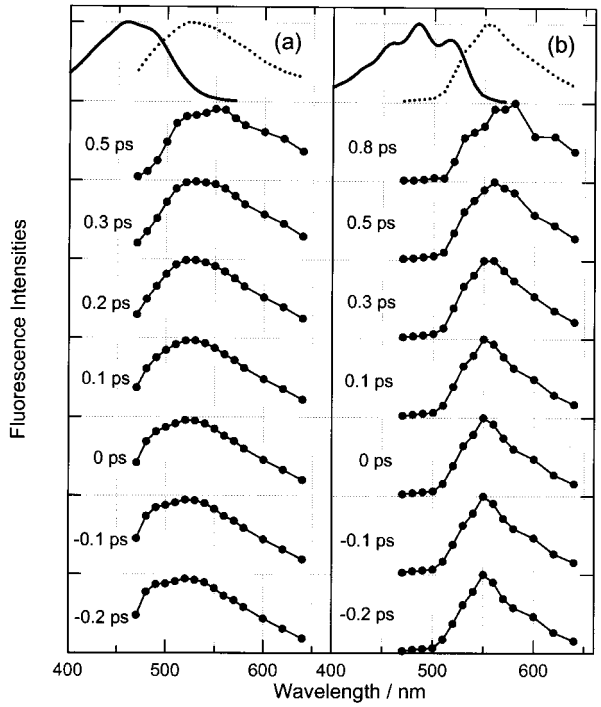

Figure 7. Normalized time-resolved fluorescence spectra of β-apo-8′-carotenal at (a) 295 K and (b) 80 K in MTHF. The steady-state absorption (full lines) and fluorescence spectra (broken lines) at the respective temperatures are also shown in the upper window.

The time-resolved fluorescence spectra at 80 K showed remarkable temperature-dependent changes in their shapes (Figure 4). A spectrum with vibrational bands appeared in the very beginning, corresponding to the mirror image of the absorption spectrum. Three peaks were recognized at approximately 510, 550, and 600 nm, showing a progression of 1430−1520 cm^{-1}, and this was responsible for the stretching vibration of the C=C bond as revealed by Raman study.[28] With an increasing delay time, the spectra became diffuse and changed peak position from $S_{2,0} \rightarrow S_{0,0}$ ($S_{2,n} \rightarrow S_{0,n}$) to $S_{2,0} \rightarrow S_{0,1}$ ($S_{2,n} \rightarrow S_{0,n+1}$), indicating that the magnitude of the displacement of the potential surface between the S_0 and S_2 states increased with time. At 0.3 ps, the spectrum showed almost the same profile as that observed at 295 K, except for the red shift by 20 nm. This behavior suggests that the excess energy equivalent to 4000 cm^{-1} was effectively transferred from the Franck−Condon active mode to the dark low-frequency mode (Table 2), resulting in an increase in the local temperature and changes in the potential surface of β-carotene. At 80 K, the time-resolved fluorescence spectrum considerably changed its shape with time. It was difficult to estimate the changes in the bandwidth and thus a time for VR on the basis of these spectra.

The fluorescence rise and decay curves and the time-resolved fluorescence spectra of β-apo-8′-carotenal are shown in Figures 6 and 7, respectively. The fluorescence lifetimes reflected the wavelength dependence as in the case of β-carotene (Table 1); they were 70 fs for 480 nm, 125−155 fs for 500−600 nm, and 170−180 fs for 620−640 nm at 295 K. At 480 nm, the resolved lifetime was much shorter than that observed for β-carotene. However, at other wavelengths, the lifetimes were comparable to those of β-carotene. In contrast to the case of β-carotene, no rise component was resolved in the fluorescence kinetics of β-apo-8′-carotenal at any of the wavelengths observed. At 80 K, the lifetimes were prolonged at every wavelength monitored: 135 fs for 480 nm, 150−200 fs for 500−600 nm, and 240−255 fs for 620−640 nm (Table 1). The rise component was not resolved as it was at 295 K, but the wavelength-dependent changes in the lifetimes, that is, long lifetimes in the long wavelength regions, were the same as those observed at 295 K.

Figure 7 shows the time-resolved fluorescence spectra under the two temperature conditions. At 295 K, a wide and featureless spectrum was observed in the initial time, and the maximum at approximately 520 nm at the earlier time was shifted to the red and reached 550 nm at 0.5 ps after the excitation. The bandwidth became somewhat narrowed with time, but its magnitude was not changed significantly. At 80 K, changes in the time-resolved spectrum were not significant; the peak observed at 550 nm in the initial time range was shifted to 570 nm at 0.8 ps after the excitation. Compared with changes in β-carotene, the spectral changes in β-apo-8′-carotenal were small. Together with the absence of the rise time for the kinetics, the processes

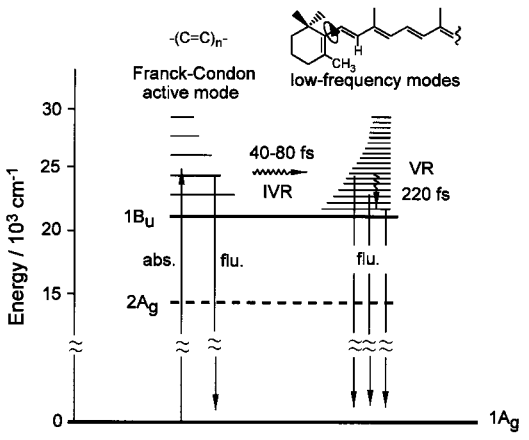

Figure 8. Relaxation processes of β-carotene in MTHF after excitation to the S_2 state with their time scales. IVR and VR stand for intramolecular vibrational redistribution and vibrational relaxation, respectively.

responsible for the spectral changes appeared to be simple, but the dynamics before this emissive process may be very fast.

On the basis of our observations, we summarized the relationship between the relaxation processes and observed phenomena in the kinetics and spectra (Table 2).

4. Discussion

In the absorption spectra of β-carotene, the vibronic structure was clearly observed especially at 80 K (Figure 2a), which can be explained by the molecular geometry. Steric hindrance between the methyl substituent at C-5 of the β-ring and the hydrogen atom at C-8 of the central chain (Figure 1) breaks the coplanarity of the molecules and markedly twists the C-5,6 double bond out of plane. This allows twisting around the C-6,7 single bond, and at this site, distribution of the twist angle is expected. At a low temperature, the distribution is shifted to a lower energy level, which made the vibronic structure clear. The spectral fine structure indicates a "local" temperature of β-carotene; as the local temperature increases, the spectrum loses its fine structure and becomes diffuse. Therefore, the temporal change in the transient fluorescence spectra should be interpreted as an excitation relaxation from the Franck−Condon active mode to the dark mode, followed by the increase in local temperature (Figure 8 and Table 2). This was also the case for half of the β-apo-8′-carotenal molecules; however the vibronic structure was not as evident, even at 80 K (Figure 2b). Therefore, it is reasonable to infer that the keto carbonyl group is much more effective for the electronic state of molecules. This might be related to a small-sized keto carbonyl group and its flexible location.[29]

The decay kinetics (Figure 3) and time-resolved fluorescence spectra (Figure 4) of β-carotene at 295 K were essentially identical to those reported previously.[17] These phenomena were common to neurosporene, a linear carotenoid found in photosynthetic bacteria,[17] thus these relaxation processes were typical of carotenoids consisting of hydrocarbon. After excitation to the S_2 state with an excess energy, there occurred energy dissipation from the Franck−Condon active mode to the inactive dark mode, that is, the IVR process occurred (Figure 8). This process was monitored by the rise time in the fluorescence rise and decay curves,[17,30] which was 40−80 fs in the middle wavelength region of the S_2 fluorescence of β-carotene at 295 K (Table 1). Recently, the $1Bu_u^-$ state has been reported to be located between the $1B_u^+$ (S_2) and 2Ag (S_1) states.[31,32] However, we attributed the rise component not to an internal conversion of $1B_u^+$ (S_2) → $1B_u^-$ but to the IVR process within the S_2 state on the basis of the following two experimental results. First, the rise component was resolved only at the middle of the fluorescence spectra, which is essentially the same as predicted for relaxation of an excess energy given to the Franck−Condon active mode.[33] If the observed rise component was due to an internal conversion from the S_2 to the lower-lying states, the rise component should be observed not only at the middle of the fluorescence spectra but also in the longer wavelength region. Second, it is reported that the fluorescence anisotropy value of β-carotene is 0.4 and does not change with time,[13] indicating that the origin of the fluorescence is the initially excited S_2 state even at the later stage. Because the $1B_u^-$ state has not yet been shown by time-resolved spectroscopy, it is not proper to compare the proposed $1B_u^-$ state with our results at this experimental stage. In addition to IVR, the second relaxation process with a time constant of 220 fs (Figure 5) was also observed by narrowing of the spectral bandwidth, and this was assigned to the VR (Figure 8).

At 80 K, the above-described relaxation processes were not necessarily reproduced in β-carotene (Figure 4b). The rise time for the kinetics was prolonged to 80−110 fs (Table 1) even though the rise times were resolved in the same wavelength region as those at 295 K. These values were 1.5−2 times longer than those at 295 K, although this does not necessarily reflect the temperature effect on the relaxation time. Because the magnitude of the time-dependent displacement of the S_2 potential surface was large at 80 K, changes in the potential surface as well as the relaxation of excess energy (i.e., IVR) should be responsible for the prolonged rise time. Therefore, the time scale of IVR at 80 K might be comparable to that at 295 K. As for the time for VR, it was hard to estimate the changes in bandwidth; however, wavelength-dependent changes in the lifetimes were pronounced under the low-temperature condition. While it is difficult to obtain conclusive information from the time-resolved fluorescence spectrum at 80 K, it is proper to infer that the VR is slower under the low-temperature condition.

The fluorescence kinetics of β-apo-8′-carotenal (Figure 6) were essentially different from those of β-carotene in the following three ways. First, the resolved lifetime at 480 nm was very short (70 fs) compared with that for β-carotene at 295 K (155 fs); however, at other wavelength regions, the lifetimes were comparable (Table 1). Second, the rise components were not necessary for the best fit of the decay curves even at the middle of the spectral region. Because the resolved decay time was comparable to β-carotene, it is reasonable to infer that the rise time might be much shorter than the time resolution of our apparatus, 30 fs. Third, the lifetimes at 80 K were longer than those at 295 K. This trend was contrary to that for β-carotene and opposite to that predicted based on the energy gap law of internal conversion.[34] Because the energy gap between the S_2 and S_1 states, ΔE_{21}, decreases at 80 K due to the temperature-insensitive S_1 state, at 80 K the internal conversion rate, which is given by an inverse of the S_2 lifetime, is expected to become smaller. However this was not the case. Our findings indicate that the energy gap law of internal conversion does not necessarily determine the decay kinetics of β-apo-8′-carotenal and that other additional factors influence these kinetics.[15,18]

As for the time-resolved spectra of β-apo-8′-carotenal, the time-dependent changes were small under the two temperature conditions (Figure 7). At 295 K, the time evolution of the transient spectra was interpreted as the dynamic red shift, instead

of the spectral narrowing observed for β-carotene. This might come from an interaction between β-apo-8′-carotenal and the solvent MTHF. It is well-known that, when the dipole moment of a solute molecule changes its direction, magnitude, or both after photoexcitation in polar solvents, the solvent molecules change their orientation around the solute, resulting in a dynamic Stokes shift. This was not the case here because the vibronic structure in the transient fluorescence spectra of β-apo-8′-carotenal became more clear with time, as was typically shown at 80 K (Figure 7b). The explanation may account for the dynamic red shift observed in the present study. As we discussed previously,[29,35] changes in the molecular geometry and relaxation kinetics in the excited state depend on a property of an intermolecular interaction, that is, whether it is attractive or repulsive, between a solvent molecule(s) and a solute carotenoid(s). In MTHF, an attractive interaction between an oxygen atom of MTHF and a hydrogen atom of the keto carbonyl group of β-apo-8′-carotenal is dominant and therefore a large conformation change is expected in the excited state. The observed red shift can be explained by dynamic changes in the molecular geometry. This process was restricted under the low-temperature condition, and thus, at 80 K, a clear vibrational structure was observed late after the excitation.

Through measurements of absorption and fluorescence spectra of a short polyene aldehyde all-*trans* retinal at low temperature, Christensen and Kohler[20] concluded that conformational disorder induces broadening of its spectral feature, and this idea is accepted widely. Therefore, it is expected for the polyene aldehydes that a large number of conformers exist in solution and that the distribution is altered by excitation, resulting in time-dependent changes in transient fluorescence spectra. However, the spectral profile of β-apo-8′-carotenal and its temperature dependence are different from those of retinal; in the absorption spectra of β-apo-8′-carotenal, the vibronic structure was recognized at room temperature and became clear under the low-temperature condition (Figure 2b), whereas the absorption spectrum of all-*trans* retinal was remarkably diffuse even at 77 K.[20] These trends suggest that the effect of conformational disorder should not necessarily be significant for the spectral feature of a long polyene aldehyde, β-apo-8′-carotenal.

A systematic study on the optical properties of polyene aldehydes[21,22] indicates that the (n, π^*) level of the molecules with seven or eight double bonds lies close to the (π, π^*) (1Bu) level, and this is applicable to β-apo-8′-carotenal. Therefore, the presence of the (n, π^*) level might cause the relaxation processes to facilitate fast internal conversion in β-apo-8′-carotenal. In a recent study, we found that the (n, π^*) level is located below the (π, π^*) (1Bu) level by approximately 660 cm^{-1} in *n*-hexane and that the fluorescence decay kinetics is represented by a very short-lived component ($\sim$80 fs) and a short-lived component ($\sim$250 fs) the amplitude of which is quite small (4% at 520 nm, Akimoto et al., unpublished). In the polar solvent MTHF, the fluorescence kinetics showed a single-exponential decay, which was independent of temperature. This suggests that the contribution of the (n, π^*) level to the relaxation from the S_2 state depends on the solvent polarity. It is well-known that the (n, π^*) and (π, π^*) levels show different solvent effects such that increasing the solvent polarity shifts the former to a higher energy whereas the latter shifts it to a lower energy.[36] Therefore, the (n, π^*) level might be very close to (or higher than) the (π, π^*) level in MTHF, resulting in solvent-dependent relaxation kinetics. Our future studies will focus on this phenomenon.

5. Summary

We examined the relaxation dynamics of a typical carotenoid, β-carotene, and its analogue, β-apo-8′-carotenal, in 2-methyltetrahydrofuran at 80 and 295 K. The relaxation processes of β-carotene at 295 K were described by IVR and the following VR. At 80 K, these two processes were not separated because the time-dependent spectral changes were large. However, it appears that the VR was slower under the low-temperature condition on the basis of the wavelength-dependent lifetimes. The relaxation processes of β-apo-8′-carotenal were very different from those of β-carotene. The time constant corresponding to IVR was not resolved under the two temperature conditions, indicating a very fast relaxation process. The time-dependent spectral changes were not significant, indicating that the second phase involved a relatively slow process. This difference in decay kinetics was attributed to the molecular structure of the solutes and the interaction between the solutes and a solvent.

Acknowledgment. The authors thank Dr. S. Takaichi, Nippon Medical School, for his help in purification of the samples. This work was supported in part by the Grant-in-aid for Scientific Research from the Ministry of Education, Culture, Sports, Science and Technology, Japan to S.A. (Grant No. 12750721), to I.Y. (Grant No. 11223203), and to M.M. (Grant Nos. 10440240 and 11223206). Financial support from the Akiyama Foundation to S.A. is also acknowledged.

References and Notes

(1) Mimuro, M.; Katoh, T. *Pure Appl. Chem*. **1991**, *63*, 123.
(2) Frank, H. A.; Cogdell, R. J. In *Carotenoids in Photosynthesis*; Young, A., Britton, G., Eds.; Chapman and Hall: London, 1993; Chapter 8, p 252.
(3) Koyama, Y.; Kuki, M.; Andersson, P. O.; Gillbro, T. *Photochem. Photobiol*. **1996**, *63*, 243.
(4) Katoh, T.; Nagashima, U.; Mimuro, M. *Photosynth. Res.* **1991**, *27*, 221.
(5) Akimoto, S.; Takaichi, S.; Ogata, T.; Nishimura, Y.; Yamazaki, I.; Mimuro, M. *Chem. Phys. Lett*. **1996**, *260*, 147.
(6) Bautista, J. A.; Connors, R. E.; Bangar Raju, B.; Hiller, R. G.; Sharples, F. P.; Gosztola, D.; Wasielewski, M. R.; Frank, H. A. *J. Phys. Chem. B* **1999**, *103*, 8751.
(7) Zigmantas, D.; Polivka, T.; Hiller, R. G.; Sundstrom, V. *Abstracts of the 12th International Congress on Photosynthesis*; Brisbane, Australia, 2001.
(8) Hudson, B. S.; Kohler, B. E.; Schulten, K. In *Excited States*; Lim, E. C., Ed.; Academic Press: New York, 1982; Vol. 6, p 1.
(9) Shreve, A.; Trautman, J. K.; Frank, H. A.; Owens, T. G.; Albrecht, A. C. *Biochim. Biophys. Acta* **1991**, *1058*, 215.
(10) Owens, T. G.; Shreve, A. P.; Albrecht, A. C. In *Research in photosynthesis*; Murata, N., Ed.; Kluwer: Dordrecht, Netherlands, 1992; Vol. 1, p 179.
(11) Nagae, H.; Kakitani, T.; Katoh, T.; Mimuro, M. *J. Chem. Phys.* **1993**, *98*, 8012.
(12) Ricci, M.; Bradforth, S. E.; Jimenez, R.; Fleming, G. R. *Chem. Phys. Lett*. **1996**, *259*, 381.
(13) Kandori, H.; Sasabe, H.; Mimuro, M. *J. Am. Chem. Soc.* **1994**, *116*, 2671.
(14) Macpherson, A. N.; Gillbro, T. *J. Phys. Chem. A* **1998**, *102*, 5049.
(15) Mimuro, M.; Akimoto, S.; Takaichi, S.; Yamazaki, I. *J. Am. Chem. Soc*. **1997**, *119*, 1452.
(16) Mimuro, M.; Akimoto, S.; Takaichi, S.; Yamazaki, I. *Photomed. Photobiol*. **1998**, *20*, 95.
(17) Akimoto, S.; Yamazaki, I.; Takaichi, S.; Mimuro, M. *Chem. Phys. Lett*. **1999**, *313*, 63.
(18) Akimoto, S.; Yamazaki, I.; Takaichi, S.; Mimuro, M. *J. Lumin.* **2000**, *87*−*89*, 797.
(19) Akimoto, S.; Yamazaki, T.; Yamazaki, I.; Osuka, A. *Chem. Phys. Lett*. **1999**, *309*, 177.
(20) Christensen, R. L.; Kohler, B. E. *Photochem. Photobiol*. **1973**, *18*, 293.
(21) Das, P. K.; Becker, R. S. *J. Phys. Chem*. **1978**, *82*, 2081.
(22) Das, P. K.; Becker, R. S. *J. Phys. Chem.* **1978**, *82*, 2093.

(23) Mimuro, M.; Nagashima, U.; Nagaoka, S.; Nishimura, Y.; Takaichi, S.; Katoh, T.; Yamazaki, I. *Chem. Phys. Lett.* **1992**, *191*, 219.
(24) Richert, R. *Chem. Phys. Lett*. **1993**, *216*, 223
(25) Chowdhury, A.; Locknar, S. A.; Premvardhan, L.; Peteanu, L. A. *J. Phys. Chem. A* **1999**, *103*, 9614.
(26) DeCoster, B.; Christensen, R. L.; Gebhard, R.; Lugtenburg, J.; Farhoosh, R.; Frank, H. A. *Biochim. Biophys. Acta* **1992**, *1102*, 107.
(27) Sue, J.; Mukamel, S. *J. Chem. Phys*. **1988**, *88*, 651.
(28) Noguchi, T.; Hayashi, H.; Tasumi, M.; Atkinson, G. H. *J. Phys. Chem*. **1991**, *95*, 3167.
(29) Mimuro, M.; Nishimura, Y.; Takaichi, S.; Yamano, Y.; Ito, M.; Nagaoka, S.; Yamazaki, I.; Katoh, T.; Nagashima, U. *Chem. Phys. Lett*. **1993**, *213*, 576.
(30) Loring, R. F.; Yan, Y. J.; Mukamel, S. *J. Chem. Phys*. **1987**, *87*, 5840.
(31) Ritz, T.; Damjanovic, A.; Schulten, K.; Zhang, J.-P.; Koyama, Y. *Photosynth. Res.* **2000**, *66*, 125.
(32) Sashima, T.; Nagae, H.; Kuki, M.; Koyama, Y. *Chem. Phys. Lett*. **1999**, *299*, 187.
(33) Horng, M. L.; Gardecki, J. A.; Papazyan, A.; Maroncelli, M. *J. Phys. Chem*. **1995**, *99*, 17311
(34) Englman, R.; Jortner, J. *Mol. Phys*. **1970**, *18*, 145.
(35) Mimuro, M.; Nishimura, Y.; Yamazaki, I.; Katoh, T.; Nagashima, U.; *J. Lumin.* **1992**, *51*, 1.
(36) Habaerfield, P.; Lux, M. S.; Rosen, D. *J. Am. Chem. Soc.* **1977**, *99*, 6828.